

## ГЕНЕРАЦИЯ СИГНАЛА С ХАОТИЧЕСКИ ОСЦИЛЛИРУЮЩЕЙ ФАЗОЙ

© 2005 г. Л. Ларже, Э. Женен, В. С. Удальцов, С. Пуансо

Описан оптоэлектронный осциллятор, генерирующий оптический сигнал с фазой, хаотически осциллирующей во времени. Осциллятор состоит из интегрально-оптических элементов, применяемых в обычных оптических коммуникационных системах. Экспериментально продемонстрированы быстрые хаотические осцилляции фазы в диапазоне частот вплоть до десятка гигагерц при постоянной интенсивности оптического сигнала. Обсуждаются возможности использования осциллятора в качестве хаос-генератора в защищенных системах связи, а также в качестве генератора стабильных радиочастотных колебаний, частота которых зависит от параметров применяемых элементов.

Коды OCIS: 060.4250, 000.5490.

Поступила в редакцию 25.11.2004.

## OPTOELECTRONIC PHASE CHAOS GENERATOR FOR SECURE COMMUNICATION

© 2005 г. L. Larger\*, É. Genin\*\*, V. S. Udaltsov\*, S. Poinso\*

\* GTL-CNRS TELECOM, UMR FEMTO-ST 6174, Georgia Tech Lorraine, Metz, France

\*\* Laboratoire d'Optique PM Duffieux, UMR FEMTO-ST 6174, Université de Franche-Comté, Besançon CEDEX, France

E-mail: laurent.larger@georgiatech-metz.fr

An optoelectronic chaos phase generator is reported, which involves conventional integrated optics and optical telecommunication components. Fast chaotic behavior of the optical phase with a constant power optical is experimentally demonstrated over multi-GHz bandwidth. Application to secure optical communications using chaos is discussed, as well as generation of high purity RF oscillations, depending on the parameter settings.

Fast chaotic dynamics have been particularly explored in optics due to their potential application to high speed secure optical communications. They have been designed following the particular nonlinear delay feedback oscillation architecture. Within this architecture, different setups have emerged, among which the most popular ones are the external cavity semiconductor laser [1–3], the fiber laser [4], and various optoelectronic feedback oscillators [5, 6]. A recent demonstration of our group showed the possibility to encode several 10s Gb/s digital message using a chaotic optical intensity carrier [7]. Following a current trend of optical telecommunication towards the use of the optical phase for encoding information instead of the intensity, we developed a new optoelectronic oscillator generating a chaotic optical phase signal while keeping a constant optical intensity. This article reports first experimental results and potential applications for this new kind of optoelectronic oscillator.

The first section is devoted to the introduction of the general architecture of a nonlinear delay differential dynamic, while the detailed setup is described in the second section together with a nonlinear delay differential model intended to numerical simulations of the dynamical solutions. Experimental results on numerous different dynamical regimes are then reported and related to

the simulation results. We conclude finally in the last section, on potential applications in chaos based secure communications, and in the generation of high purity RF oscillations.

## 1. Nonlinear Delay oscillators

Among the numerous possible ways to generate chaos, optical nonlinear delay differential dynamics offer attractive features, especially for applications to chaos-based secure communications. Mathematically, these dynamics are described by equations that can be as simple as scalar first order differential equations:

$$x(t) + \tau \frac{dx}{dt}(t) = f[x(t-T)], \quad (1)$$

where  $x(t)$  is the dynamical variable,  $T$  is a delay,  $\tau$  is the physical response time of the dynamical process,  $f[\cdot]$  is a nonlinear function with at least one extremum.

The solutions of Eq. (1) are intrinsically evolving in an infinite phase space dimension due to the presence of a delay: the initial conditions required to determine uniquely any solution  $\{x(t)\}$  is a functional  $\{x_0(t)\}$  defined on a time of duration corresponding to the delay i. e., for  $t \in [-T, 0]$ . When high complexity is required, the delay is usually set to a value much larger than the



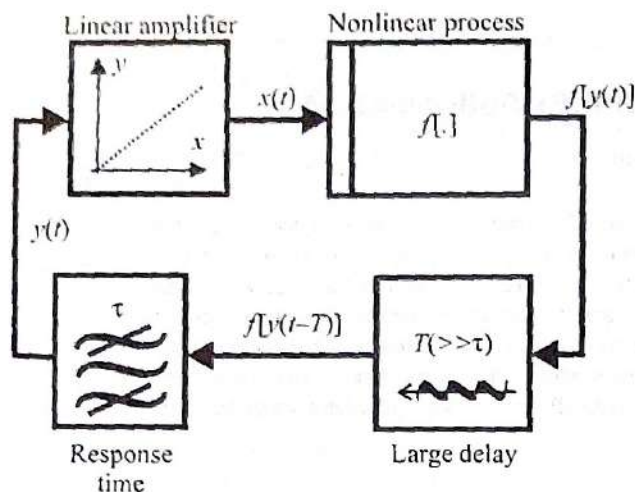


Fig. 1. Block-diagram of a nonlinear delayed differential oscillator.

slowest physical response time of the system. The infinite phase space dimension allows practically for high complexity chaotic solutions, which finite attractor dimension can be as high as several hundreds (of the order of the ratio  $T/\tau$ ). In terms of confidentiality (for applications to secure chaos communications), this property has been found to be a necessary condition, since numerous chaos encryption systems using low dimensional attractors have been already cracked.

The general principle of nonlinear delay differential dynamics is depicted in Fig. 1 from a system point of view. The oscillator is organized in a single feedback loop system consisting of the following elements:

1. A nonlinear function with at least one extremum. The number of extrema actually used in a given dynamical regime is fixed by the amplitude of the nonlinear block input.
2. The latter amplitude is directly related to the feedback loop gain, which is represented in the schematic by the tuning efficiency of variable  $x$  into variable  $y$ .
3. A delay line performing a constant time shift over the whole frequency components of the chaotic signal

(non dispersive delay line). It can be easily performed in Optics with optical fibers, due to their huge bandwidth.

4. A dynamic limitation process performed here by a physical response time  $\tau$ . When the dynamical process is of a first order as it is the case in Eq. (1), a single physical response time is involved. Wide band oscillators however usually involve several cut-off frequencies, and they also involve a band pass behavior instead of a low pass one as reported in Eq. (1).

Following the architecture depicted in Fig. 1, we performed several optical as well electronic chaos generators [8–12]. Each setup is based on different physical principles in order to realize a nonlinear function. The setup reported in this article involves not only a different physical principle to generate a nonlinear process (tuning of a ring resonator), but it also introduces a significantly new approach from the dynamical system point of view, in the sense it combines dynamical effects in both the RF domain (fast electrooptic modulation) and the optical domain (transient phenomena in the long optical ring cavity).

## 2. Phase chaos setup and principle of operation

The experimental setup is depicted in Fig. 2. It consists of an optoelectronic feedback loop comprising the following components, most of which are standard optical telecommunication devices:

a. An integrated LiNbO<sub>3</sub> electrooptic phase modulator, with a modulation bandwidth of 12 GHz, and a half wave voltage  $V_\pi = 5,5$  V.

b. A fiber ring resonator [13] made with a 2x2 50/50 fiber coupler, which output port 4 is spliced with the input port 2. The ring length is  $L = 1,25$  m, thus leading to a free spectral range of about  $FSR = 160$  MHz. A polarization controller is used inside the loop to select only one polarization eigenmode of the cavity. Due

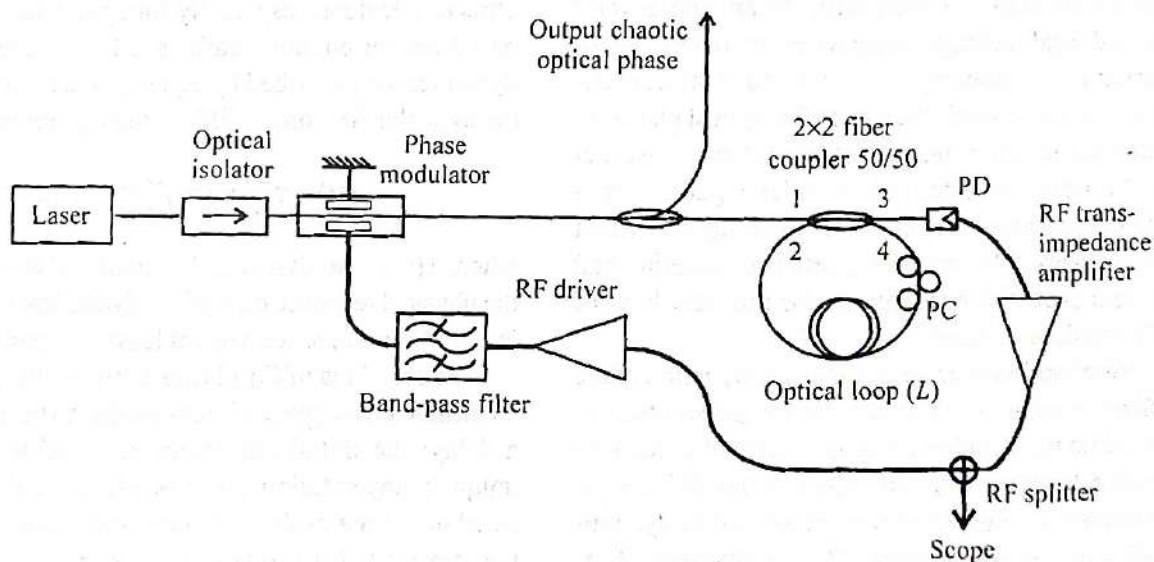


Fig. 2. Experimental setup. PD – photodiode, PC – polarization controller.



to the coupling ratio, and due to the unavoidable coupling and cavity losses, the cavity finesse is usually low; it was measured to be  $F = 8.4$ .

c. A fast RF wide band (10 kHz–15 GHz) preamplified ( $S = 2$  V/mW) photodiode, which converts into an electronic signal any intensity fluctuation at the remaining ring cavity output port (port 3).

d. A wide band (30 kHz–26 GHz) high gain RF driver (max. output 26 dBm,  $K = 18$  dB gain), which output is connected to the RF port of the phase modulator, thus closing the optoelectronic feedback loop. This second electronic amplifier is needed in order to allow electrooptic modulation amplitude which covers at least 2 half wave voltages ( $V_\pi$ ) of the phase modulator, thus leading to a multiple extrema modulation of any optical interferometer using this phase modulation (which means practically a strong nonlinear transfer function of the interferometer; as already described, the interference here performed by the ring cavity).

e. The optical input of the phase modulator is seeded by an ultra stable DFB fiber laser at 1.55  $\mu\text{m}$  (linewidth smaller than 20 kHz, and central wavelength fluctuations better than 1 MHz i. e., 0.01 pm). Such stability is practically required due to the extremely long length of the optical cavity.

The general principle of operation of the whole optoelectronic oscillator can be interpreted as follow. Starting from the internal noise of the oscillator, fast electronic amplitude fluctuations generate a phase modulation that is converted into intensity fluctuations at the ring cavity output, because the fluctuations can be faster than a round trip of the cavity. The initial fluctuations are hence amplified within an optoelectronic feedback path, through the phase/intensity nonlinear conversion, together with the optoelectronic sensitivity of the detection, with the electronic amplification, and with the electrooptic tuning rate.

Assuming the optoelectronic, electronic, and electrooptic parts are operating linearly, and that they mainly fix the feedback gain and the maximum speed of the fluctuations (filtering effect due to the electronic bandwidth of the feedback), the dynamical law ruling the oscillations can be written in first approximation by the following nonlinear delay integro-differential equation (which differs from Eq. (1)):

$$\tau_2 \frac{d\Phi}{dt}(t) + \left(1 + \frac{\tau_1}{\tau_2}\right) \Phi(t) + \frac{1}{\tau_1} \int_{-\infty}^t \Phi(\theta) d\theta = GP_3(t), \quad (2)$$

where  $\tau_1$  and  $\tau_2$  are the time constants corresponding respectively to the low and high cut-off frequencies of the electronic feedback,  $\Phi(t)$  is the optical phase due to the electrooptic phase modulator,  $P_3(t)$  is the optical intensity detected at the output port 3 of the fiber coupler, and  $G = \pi KS/V_\pi$  is the overall conversion factor (opto-

electronic gain) from intensity fluctuations into phase modulation.

The quantity  $P_3(t)$  is obtained from the instantaneous fiber ring cavity equations (interference between the input amplitude  $E_1$  and the feedback amplitude  $E_2$ ), which gives the envelop of the output electric field at port 3 and 4 of the fiber coupler:

$$\begin{aligned} E_3 &= \rho \left( \sqrt{\kappa} E_1 + i \sqrt{1 - \kappa} E_2 \right), \\ E_4 &= \rho \left( i \sqrt{1 - \kappa} E_1 + \sqrt{\kappa} E_2 \right), \end{aligned} \quad (3)$$

where  $\kappa$  is the coupling ratio,  $\rho$  describes the coupler losses  $E_3(t) = \sqrt{P_3(t)} e^{i\phi_3(t)}$ , and  $E_2(t)$  is actually the feedback amplitude that can be written as the output amplitude at port 4 delayed by  $T$   $E_4(t - T) = E_{4T} = \sqrt{P_{4T}(t)} e^{i\phi_{4T}}$ , phase shifted by the static ring cavity accumulated phase  $\Phi_L = 2\pi nL/\lambda$ , and attenuated due to the cavity losses:

$E_2(t) = \sqrt{\gamma} E_{4T} e^{i\Phi_L(t)}$  (the subscript  $T$  is representative of a delayed quantity i. e.,  $x_T(t) = x(t - T)$ ). Assuming then the input beam is only phase-modulated by the electrooptic effect, one has  $E_1(t) = \sqrt{P_0} e^{i\Phi(t)}$ . The optical intensity at port 3 is finally given by:

$$\begin{aligned} P_3(t) &= \rho P_0 \left[ \kappa + (1 - \kappa) \gamma \frac{P_{4T}}{P_0} - \right. \\ &\quad \left. - 2 \sqrt{\gamma \kappa (1 - \kappa)} \frac{P_{4T}}{P_0} \sin(\phi_{4T} + \Phi_L - \Phi(t)) \right]. \end{aligned} \quad (4)$$

In order to calculate  $P_3$ , one would actually needs to find  $P_4$  and  $\phi_4$ , which are obtained according to a 2-D discrete mapping (the iteration step corresponds to the cavity round trip  $T$ ) combined with the continuous time phase fluctuations  $\Phi(t)$ :

$$\begin{aligned} P_4(t) &= \rho P_0 \left[ 1 - \kappa + \kappa \gamma \frac{P_{4T}}{P_0} + \right. \\ &\quad \left. + 2 \sqrt{\gamma \kappa (1 - \kappa)} \frac{P_{4T}}{P_0} \sin(\phi_{4T} + \Phi_L - \Phi(t)) \right], \\ \phi_4(t) &= \Phi(t) + \frac{\pi}{2} - \\ &\quad - \arctg \left[ \frac{\sqrt{\gamma \kappa P_{4T}} \cos(\phi_{4T} + \Phi_L - \Phi(t))}{\sqrt{(1 - \kappa) P_0} + \sqrt{\gamma \kappa P_{4T}} \sin(\phi_{4T} + \Phi_L - \Phi(t))} \right]. \end{aligned} \quad (5)$$

With the previous static and dynamic relations, it was possible to integrate with a 4th order Runge-Kutta scheme the differential law in Eq. (2), and to calculate numerous different dynamical regimes for various



experimental parameter conditions e. g., the central laser wavelength  $\lambda$  (finely tuned through temperature control), and the global optoelectronic feedback loop gain (controlled through the laser power  $P_0$  or through a tunable gain RF amplifier). The latter parameter corresponds numerically to the dimensionless quantity  $\beta = G\rho P_0/2$ .

### 3. Experimental and numerical results

When increasing the optoelectronic feedback gain through the tunable gain of the RF driver, it is possible to obtain numerous dynamical regimes (see time traces in Fig. 3), as typically observed in other nonlinear delayed feedback oscillators. The observed variable is a fraction of the electronic feedback signal at the output of an electronic power divider. For low feedback gain, no oscillation is able to start, and a stable zero fixed point is observed. At a given threshold, fast RF oscillations of a few 100 MHz (corresponding to a rational number of the fundamental frequency  $1/T$ ) are obtained (Fig. 3a); their amplitudes are growing with the feedback loop gain. Further increasing the electronic feedback gain leads to distorted oscillations (Fig. 3b) thus broadening the spectrum, but still exhibiting frequency components locked to  $1/T$ . Above another higher feedback gain threshold, no locking is observed, but a strongly chaotic oscillation is obtained (Fig. 3c), which spectrum extends over a bandwidth related to that of the electronic feedback (from a few 10 s of kilohertz up to approximately 6 GHz, Fig. 3d). All the previous regimes have been obtained with  $\Phi_L = 0,34$  rad (which is adjusted through the laser wavelength); different but qualitatively similar bifurcation behaviors are observed experimentally for other tuning of the ring cavity operating point. Those dynamical regimes can be compared with the ones obtained numerically with the theoretical model described by Eqs. (2), (4) and (5). A very good qualitative agreement is found, thus validating the theoretical model. It can be also noticed that for nearly all the possible operating points ( $\Phi_L$ -values), a strong loop gain leads to chaotic regimes similar to the one shown in Figs. 3c and 3d (from the spectral and statistical properties), but different from the determinism point of view (they exhibit different characteristic dynamical properties, such as Lyapunov exponents). Those regimes are of special interest in our initial goal: designing a wide band optical phase chaos generator for secure communications.

However, for some restricted particular central laser wavelength adjustments, a high purity unexpected RF oscillation at 13,9 GHz was observed (see Fig. 4). The spectral width of this high frequency oscillation could not be determined, since it reached the resolution of our RF spectrum analyzer (3 kHz). However, this pure sinusoidal oscillation has not been obtained numerically,

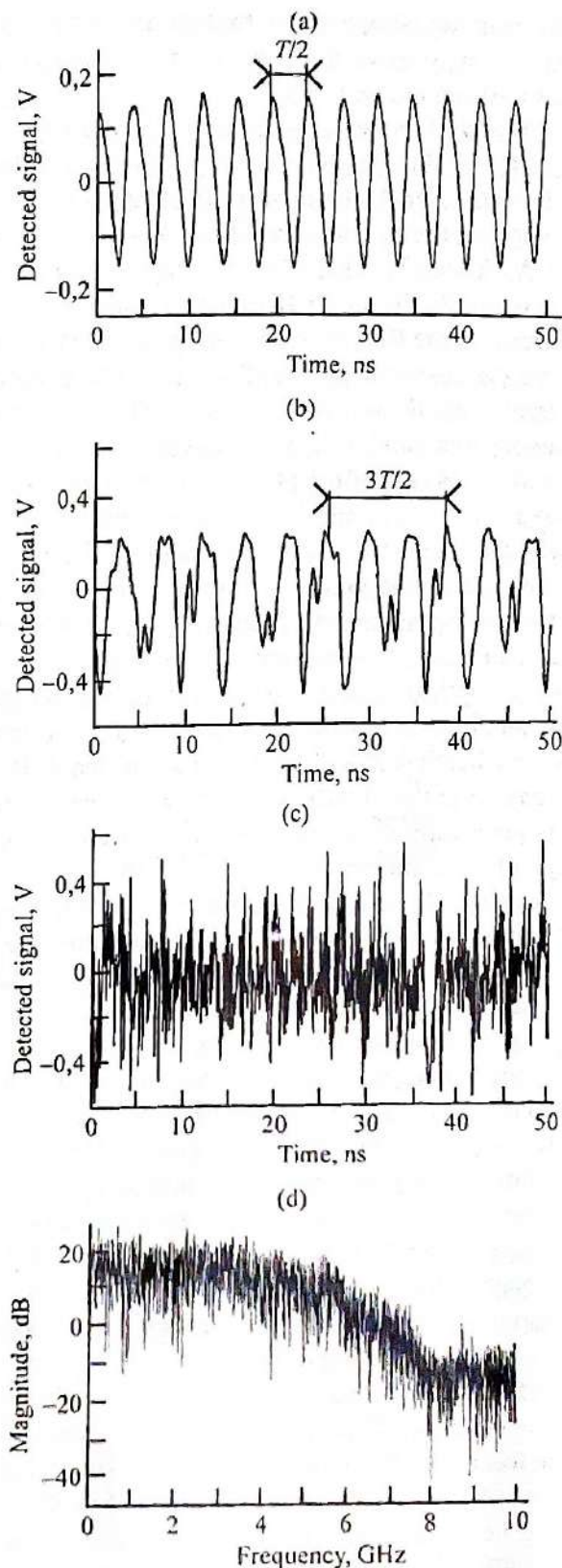


**Fig. 3.** Time traces of different dynamical regimes. (a) first periodic regime,  $\beta = 2,2$ ; (b) distorted oscillation containing subharmonic oscillations,  $\beta = 2,7$ ; (c) fast oscillations of high complexity chaotic regime,  $\beta = 3,8$ ; (d) spectrum of the chaotic regime,  $\beta = 3,8$ .

which might be explained by the possible strong saturation of the RF driver under the corresponding operation conditions. Such a high purity RF optoelectronic oscillator could be of great interest for a new genera-



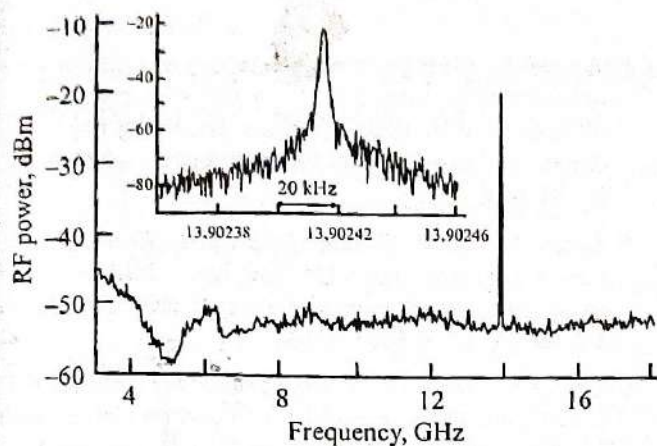


**Fig. 4.** Spectrum of the high purity RF harmonic regime.

tion of RF oscillators in the frequency range above 10 GHz, which arose recently in similar optoelectronic architecture by means of intensity electrooptic modulators [14].

#### 4. Conclusions and potential applications

A nonlinear dynamics operating with the variable "optical phase" was reported. Under proper parameter settings, a wide band chaotic oscillation covering several gigahertz was observed, which could be then used for high bit rate chaos based secure optical communica-

tion. Typical emitter-receiver architecture is proposed in Fig. 5 [15]. The message is encoded using a power combiner in the electronic part of the oscillator, superimposing a small signal information to the chaotic electronic feedback signal. The transmitted light beam corresponds to the output of a fiber coupler placed after the electrooptic phase modulator; it consists of a constant intensity light beam, phase modulated with a large amplitude chaotic part, superimposed to a small amplitude message part. At the receiver side, a twin optoelectronic oscillator is used to generate a synchronized chaos [16]. When accurate synchronization can be achieved, the chaotic part of the received phase modulation can be removed, thus leading to the message recovery. Work is in progress to implement experimentally the encoding and decoding architecture.

Out of the chaotic regime, many different other dynamical behaviors were reported with the same setup, but operating with different parameter settings. A good qualitative agreement was noticed between theory and experiments. Unusual single frequency oscillations at 13,9 GHz were also observed, although not obtained from the numerical simulations. Strong RF amplifier saturation is suspected, which was not taken into account in the model. Work is in progress to characterize and improve the stability of this pure sinusoidal high frequency oscillation, and to measure precisely its purity with appropriate equipments.

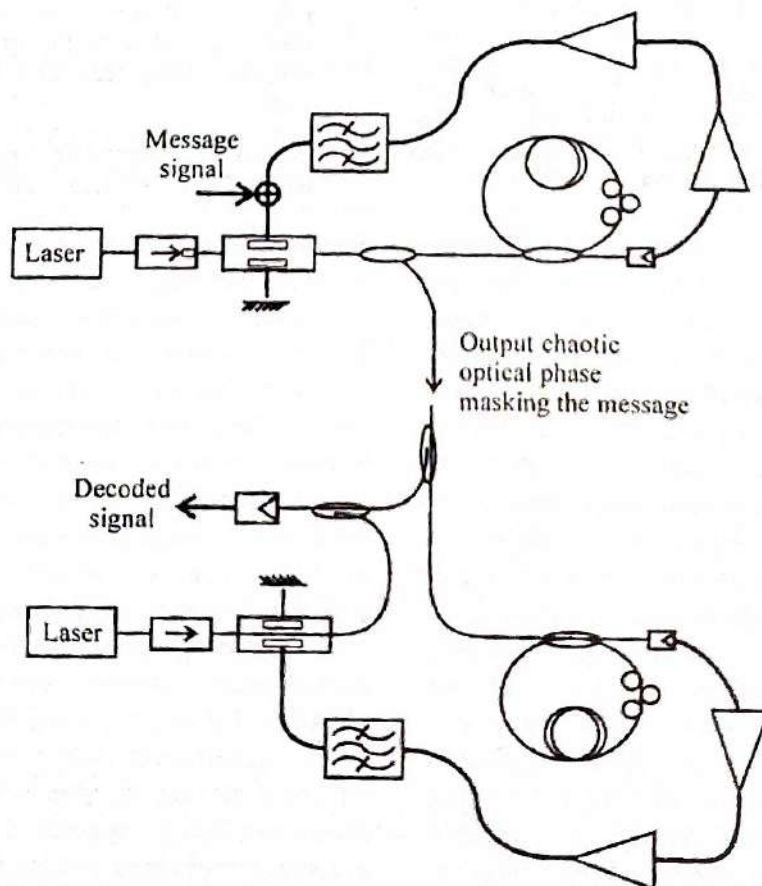


**Fig. 5.** Encoding and decoding system using the chaotic regime as an information masking carrier.



## Aknowledgement

The participation of V.S. Udaltsov was supported by the Centre National de la Recherche Scientifique (CNRS), France. This work was funded by the EEC (Contract IST-2000-29683, OCCULT), and the Fond National pour la Science of the French Ministry of Research ("Transchaos" contract, ACI-SI).

## REFERENCES

1. *Mirasso C., Colet P., Garcia-Fernandez P.* Synchronization of chaotic semiconductor lasers: Application to encoded communications // *IEEE Phot. Techn. Lett.* 1996. V. 8. № 2. P. 299–301.
2. *Annovazzi-Lodi V., Donati S., Sciré A.* Synchronization of chaotic lasers by optical feedback for cryptographic applications // *IEEE J. Quant. Electron.* 1996. V. 32. P. 953.
3. *Fischer I., Liu Y., Davis P.* Synchronization of chaotic semiconductor laser dynamics on subnanosecond time scales and its potential for chaos communication // *Phys. Rev. A.* 2000. V. 62. P. 011801(R).
4. *VanWiggeren G.D., Roy R.* Communication with chaos lasers // *Science.* 1998. V. 279. P. 1198–1200.
5. *Goedgebuer J.-P., Larger L., Porte H.* Optical cryptosystem based on synchronization of hyperchaos generated by a delayed feedback tunable laser diode // *Phys. Rev. Lett.* 1998. V. 80. № 10. P. 2249–2252.
6. *Tang S., Liu J.M.* Synchronization of high-frequency chaotic optical pulses // *Opt. Commun.* 2001. V. 26. № 9. P. 596–598.
7. *Gastaud N., Poinot S., Larger L., Merolla J.-M., Han-na M., Goedgebuer J.-P., Malassenet F.* Electrooptic Chaos for Encrypted Multi-Gb/s Optical Transmissions // *Electron. Lett.* 2004. V. 40. P. 898–899.
8. *Larger L., Goedgebuer J.-P., Merolla J.-M.* Chaotic oscillator in wavelength: a new setup for investigating differential difference equations describing non linear dynamics // *IEEE Journ. Quant. Electron.* 1998. V. 34. P. 594–601.
9. *Larger L., Lee M.-W., Goedgebuer J.-P., Erneux T., Elfle W.* Chaos in coherence modulation: bifurcations of an oscillator generating optical delay fluctuations // *JOSA B.* 2001. V. 18. P. 1063–1068.
10. *Larger L., Udaltsov V.S., Goedgebuer J.-P., Rhodes W.T.* Chaotic dynamics of oscillators based on circuits with VCO and nonlinear delayed feedback // *Electron. Lett.* 1999. V. 36. P. 199–200.
11. *Goedgebuer J.-P., Levy P., Larger L., Chen C.C., Rhodes W.T.* Optical Communication With Synchronized Hyperchaos Generated Electrooptically // *IEEE Journ. Quant. Electron.* 2002. V. 38. P. 1178–1183.
12. *Genin E., Larger L., Goedgebuer J.-P., Lee M.W., Ferrière R., Bavard X.* Chaotic oscillations of the optical phase for high-speed secure communications // *IEEE Journ. Quant. Electron.* 2004. V. 40. P. 294–298.
13. *Imai Y., Tamura T.* Coherence effect on nonlinear dynamics in fiber-optic ring resonator // *Opt. Commun.* 2001. V. 195. P. 259–265.
14. *Yao X.S.* Multiloop optoelectronic microwave oscillator with a wide tuning range // *US patent.* № 5, 777, 778. 1998.
15. *Udaltsov V.S., Goedgebuer J.-P., Larger L., Rhodes W.T.* Communicating with optical hyperchaos: information encryption and decryption in delayed nonlinear feedback systems // *Phys. Rev. Lett.* 2001. V. 86. № 9. P. 1892–1895.
16. *Pecora L.M., Carroll T.L.* Synchronization in chaotic systems // *Phys. Rev. Lett.* 1990. V. 64. № 8. P. 821–824.